Oscillatory Failure Case Detection for Aircraft using Non-Homogeneous Differentiator in Noisy Environment

J. Cieslak[*], D. Efimov[**], A. Zolghadri[*], D. Henry[*], P. Goupil [£]
[*] Univ. Bordeaux, IMS lab, 351 cours de la Libération, F-33400 Talence, France
e-mail: {jerome.cieslak / ali.zolghadri / david.henry}@ims-bordeaux.fr
[**] INRIA - LNE, Parc Scientifique de la Haute Borne 40, avenue Halley Bât.A, Park Plaza, 59650 Villeneuve d'Ascq, France, {denis.efimov@inria.fr}
[£] EYCC Flight Control System, Airbus Operations S.A.S., Toulouse, France, philippe.goupil@airbus.com

Abstract: In this paper, the problem of Oscillatory Failure Case (OFC) detection in aircraft servo-loop control surfaces is addressed. OFC leads to strong interactions with loads and aeroelasticity and consequently must be detected as quick as possible. This paper proposes a hybrid monitoring scheme developed during ADDSAFE[1] project for robust and early detection of such unauthorized oscillatory events. More precisely, a hybrid robust non-homogeneous finite-time differentiator is firstly used to provide bounded and accurate derivatives in noisy environment. Fault reconstruction is next made by solving on-line a nonlinear equation using a gradient descent method. The detection is finally done by the decision making rules currently used for in-service Airbus A380 airplane. Robustness and performance of the proposed scheme are tested using a high fidelity benchmark and intensive Monte Carlo simulations based on several flight scenarios specified in ADDSAFE. The performance indicators highlight that the proposed scheme can be a viable solution for realistic issues. Note that the term "viable" covers some important aspects which are often under-estimated (or missing) in the classical academic publications: tuning, complexity of the design, real time capability, etc.

1. Introduction

1.1. Motivations

Among a number of research areas, FDI (Fault Detection and Isolation) and FTC (Fault Tolerant Control) have been identified as a challenging thematic field for the control of large scale and complex systems. With the increasing acceptance

[1] ADDSAFE is a European collaborative project supported by the European Seventh Framework Program: Advanced Fault Diagnosis for Sustainable Flight Guidance and Control. http://addsafe.deimos-space.com

of the FDI/FTC technology in practice [1-4] and successful applications across the industrial areas (see [6, 27] to name a few), the current development in the FDI/FTC area consists of solving challenging monitoring, diagnosis and reconfiguration problems for real applications. The work presented in this paper belongs to this trend. It has been undertaken within the European FP7 project named ADDSAFE [7]. This project aims at developing innovative FDI techniques for model-based Fault Detection and Diagnosis (FDD) of flight control system. The final goal is to contribute to overall aircraft structural design optimization. This will help to make the future airplanes lighter, that is a key objective for the manufactures to improve their performance and to limit their environmental footprint.

To provide some alternative solutions in this trend, the problem of Oscillatory Failure Case (OFC) detection for aircraft is addressed here. An OFC is an abnormal oscillation of a control surface due to component malfunction in control surface servo-loops. This signal, of unknown amplitude and frequency, is propagated through the control loop to the control surface, and it could excite the airplane structure producing structural loads. OFCs could result in high loads and vibrations particularly if they resonate at a natural frequency of the aircraft structure [1-5]. For example, an OFC occurring on an aileron creates inertial moment and aerodynamic forces (hinge moment). Moreover, consequently to the control surface oscillation, vibrations appear on the wing leading to the wing bending and loads are generated very quickly on the wing and then on the whole aircraft. This is why it is very important to detect OFC at a very early stage, before loads exceed the specified design loads, as the aircraft is designed to be used inside a given load envelope . If OFCs of given amplitude cannot be detected and accommodated in time, this amplitude must be considered for load computations. If the result of this computation falls outside the load envelope, then it is necessary to reinforce the structure. So, in order to avoid reinforcing the structure and consequently to save weight, a low amplitude OFCs must be detectable at a very early stage.

In this context, the goal of this work is to develop a robust model-based monitoring strategy to detect such failures with small amplitude at an early stage. A potential detection method should comply with stringent operational conditions in terms of trade-offs for detection performance, fault coverage, robustness, computational burden (memory storage, CPU load) and design complexity. It must also offer the possibility of reuse (or building around it), with adequate design and tuning engineering tools. Use of approaches with restricted high-level tuning parameters is very important to reduce the test phase needed for aircraft algorithm certification procedure. The procedure proposed in this paper provides such a framework with tunable design parameters for easy management of trade-offs.

1.2. Antecedents and paper contribution

There exist many solutions available in the open literature. In [1], an industrial validated and implemented OFC detection strategy is proposed. A nonlinear actua-

tor model is used to generate a residual on which the failure is detected by oscillation counting. Based on the hydraulic actuator model, a nonlinear observer-based strategy using the oscillation counting of [1] is proposed in [3]. The main difficulty consists in finding a systematic tuning for observation gains. Other solutions can be also found in [8, 9]. Due to a certain level of robustness against disturbances, excellent scalability and a finite time of convergence, sliding-mode techniques have received considerable attention in this area [10-16]. Tools for linear systems are considered in [17-21], an adaptive observer approach can be found in [22]. An adaptive sliding mode super twist algorithm based on Lyapunov approach is also proposed in [23]. Because of the noisy situation in which the actuator operates, the gain of super twist algorithm is adapted to obtain a good fault reconstruction.

The proposed solution of this paper is addressed in the framework of unknown input estimation problem for fault reconstruction. To overcome the limitations of existing fault estimation methods in noisy environment, a hybrid robust non-homogeneous finite-time differentiator is firstly used to provide accurate derivatives in noisy environment. The global boundedness and accuracy of derivatives can be guaranteed [24]. Fault reconstruction is next made by solving on-line a nonlinear equation using a gradient descent method [25] to have a low computational load. This fault reconstruction algorithm is finally associated with the decision making rules as currently used for in-service Airbus A380 airplane [1]. The objective of this paper is to demonstrate that the proposed hybrid differential observer could be a good and technologically viable candidate to improve the fault detection performance for OFC in control surface servo-loops. Note that the developed scheme has been adapted to satisfy constraints (low computational load, restricted symbol library [26], …) of implementation in a Flight Control Computer (FCC). More precisely, the proposed monitoring scheme has been coded at a very basic level since embedded algorithm cannot be implemented.

Structure of the paper: Some preliminaries about the industrial issue are introduced in section 2. The fault detection and isolation technique is formulated in section 3. Finally, section 4 presents simulation results based on a high-fidelity non-linear Matlab/Simulink benchmark provided by Airbus and a Monte Carlo campaign based on Functional Engineering Simulator (FES) packages which have been developed during ADDSAFE project.

Notations: Euclidean norm for a vector $\mathbf{x} \in R^n$ will be denoted as $|\mathbf{x}|$, and for a measurable and locally essentially bounded input $u : R_+ \to R$ ($R_+ = \{\tau \in R : \tau \geq 0\}$) the L_∞ norm is denoted as $\| u \|_{[t_0,T]} = \operatorname{ess\,sup}\{|u(t)|, t \in [t_0, T]\}$, if $T = +\infty$ then we will simply write $\| u \|$. We will denote as $\mathcal{L}_\infty$ the set of all inputs u with property $\| u \| < +\infty$. Strictly increasing functions $\sigma : R_+ \to R_+$ with the property $\sigma(0) = 0$ form the class $\mathcal{K}$. Denote the sequence of integers $1, .., k$ as $\overline{1,k}$.

2. Problem definition

2.1. OFCs in control surface servo-loop

The faulty components can be located inside the analog inputs/outputs, the position sensors or the actuators. In this paper, only OFCs located in the servo-control loop of the moving surfaces are considered, i.e. OFCs located between the flight control computer and the actuator [1], see Fig. 1. Consequently, the failure impacts only one control surface. Furthermore, the control surface sensor (see Fig. 1) will be not considered available in the following developments since the proposed monitoring scheme must be valid for both elevator and aileron surfaces.

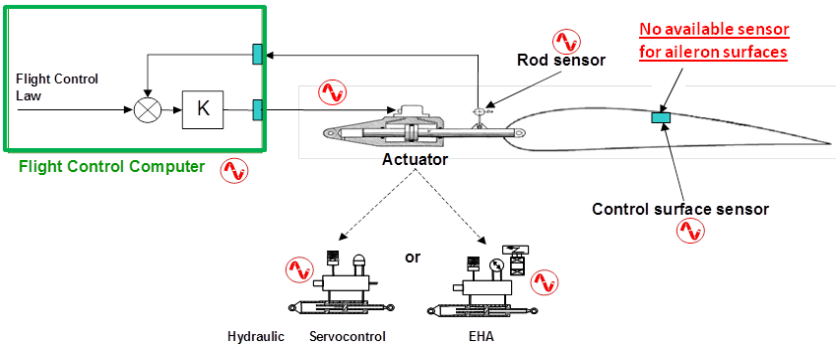

Figure 1: OFC source location within the actuator control loop.

In control surface servo-loop, two types of OFC can be identified: liquid OFCs manifest their presence as the sum of the original signal and an oscillation while solid OFCs are oscillations completely substituting the original signal. It follows

$$\begin{cases} u(t) = u_0(t) & fault-free\ \ situations \\ u(t) = u_0(t) + f_{liq}(t) & liquid\ \ fault \\ u(t) = u_0(t) + f_{sol}(t) & solid\ \ fault \end{cases} \quad (1)$$

where u_0 is the fault-free part of control. $f_{liq}(t) = f_{harm}(t)$ and $f_{sol}(t) = f_{harm}(t) - u_0(t)$ where $f_{harm}(t)$ is a harmonic fault signal.

OFCs are considered as harmonic signals with frequency and amplitude uniformly distributed over the frequency range 0.1—10 Hz. Beyond 10 Hz, OFCs have no significant effects because of the low-pass behavior of the actuator. The time detection is expressed in period numbers which means that the time allowed for detection is not the same, depending on the failure frequency.

2.2. Servo-controlled actuator modeling

The core element of the proposed model-based monitoring scheme is the servo-controlled nonlinear actuator model. The corresponding equation gives the actua-

tor rod speed as a function of the hydraulic pressure delivered to the actuator and the forces applying on the control surface and reacted by the actuator. The actuator rod speed can be expressed as the rod speed command, weighted by two main contributor factors which are aerodynamic forces and the servo control load in damping mode (of the passive actuator in the case of two actuators [1]). The actuator rod speed for a hydraulic servo control is expressed as [1]

$$\dot{y}(t) = K_{ci}K(u(t) - y(t))\sqrt{\frac{\Delta P(t) - \frac{F_{aero}(t) + F_{damp}(t)}{S}}{\Delta P_{ref}}}$$

where:
- ΔP is the hydraulic pressure delivered to the actuator.
- ΔP_{ref} is the constant differential pressure used to study actuator performance with the servo valve fully opened.
- $F_{aero}(t)$ represents the aerodynamic forces applying on the control surface. This term is an important parameter of the actuator model. The corresponding aerodynamic model is known. It can be very complex if the nonlinear effects are included. However, for industrial reasons and as it is not of primary interest in this work to give the exact expression of the model, it is not detailed in this paper.
- $F_{damp}(t)$ represents the servo control load of the adjacent actuator in damping mode: $F_{damp}(t) = K_a(t)\dot{y}(t)^2$
- $K_a(t)$ and $\dot{y}(t)$ are the actuator damping coefficient and the rod speed.
- K and K_{ci} are simple and double slope known gains used to make conversion. Note that K and K_{ci} can be more complex (use of lookup tables or gain scheduling techniques) to model actuators in more details.
- S is the actuator piston surface area.
- $u(t)$ is the actuator command signal provided by the flight control law.

The actuator rod speed (for the servo-controlled hydraulic actuator, see Fig. 1) can thus be expressed by the following local model:

$$\dot{y}(t) = K_1(u(t) - y(t))\sqrt{\frac{K_2}{\Delta P_{ref} + K_3(u(t) - y(t))^2}} \tag{2}$$

$$\psi(t) = y(t) + v(t) \tag{3}$$

where $K_1 = K_{ci}K$, $K_2 = \Delta P - (F_{aero}/S)$ and $K_3 = (K_a(K_{ci}K)^2)/S$. $\psi(t)$ is the signal available for measurements, where $v : R \to [-\lambda_0, \lambda_0]$, $0 < \lambda_0 < +\infty$ is the bounded noise.

3. Hybrid differential observer

According to the discussion of section 1.2, the structure of the proposed monitoring scheme is given in Fig. 2. In this section, we propose to give the mathematical developments, which prove the boundedness, accuracy of derivate estimates, fault reconstruction and OFC detection in noisy environment.

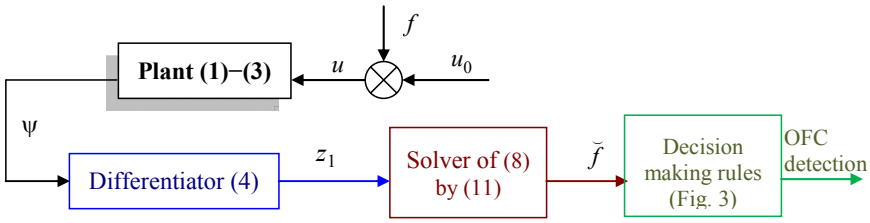

Figure 2: Structure of the hybrid monitoring scheme

3.1. Boundedness and accuracy of derivatives

Consider the servo-controlled nonlinear SISO model of (2). Without loss of generality, (2) can be rewritten according to

$$\dot{y}(t) = F(t, y, u),\ t \geq 0,$$

where

$$F(t, y, u) = K_1(u(t) - y(t))\sqrt{\frac{K_2}{\Delta P_{ref} + K_3(u(t) - y(t))^2}}$$

In this case (n=1), a variant of super-twisting differentiator [24] is used to provide robust derivative estimate against a non-differentiable noise of any amplitude. Finite-time convergence and accuracy of derivatives can be computed. The sliding mode differentiator is given by

$$\dot{z}_0 = -\alpha\sqrt{|z_0 - \psi(t)|}\,sign[z_0 - \psi(t)] + z_1, \alpha > 0, \quad (4a)$$

$$\dot{z}_1 = -\beta\,sign[z_0 - \psi(t)] - \chi\,sign(z_1) - z_1,\ \beta > \chi \geq 0, \quad (4b)$$

where $z_0 \in R$, $z_1 \in R$ are the state variables of the system (4). α, β and χ are the tuning parameters. The variable $z_0(t)$ serves as an estimate of the function $y(t)$ and $z_1(t)$ converges to $y'(t)$. Therefore, (4) has the input $\psi(t)$ and the output $z_1(t)$.

According to (3), the system (4) is discontinuous and affected by the disturbance v. First, we would like to prove that the system has bounded trajectories. Second, we would like to show that the accuracy of derivatives estimation depends continuously on the noise amplitude of v. Introducing variables $e_0 = z_0 - y$, $e_1 = z_1 - y'$, the system (4) can be rewritten as follows:

$$\dot{e}_0 = -\alpha\sqrt{|e_0|}\,sign[e_0] + e_1 + \delta_0(t), \quad (5a)$$

$$\dot{e}_1 = -\gamma(t)\,sign[e_0] - \chi\,sign[e_1] - e_1 + \delta_1(t), \quad (5b)$$

$$\delta_0(t) = \alpha(\sqrt{|e_0|}\,sign[e_0] - \sqrt{|e_0 - v(t)|}\,sign(e_0 - v(t))),$$

$$\delta_1(t) = \beta\big(sign(e_0) - sign(e_0 - v(t))\big),$$

where δ_0, δ_1 are the disturbances originated by the noise v presence, $\gamma(t) = \beta + (y'(t) + y''(t) - \chi(sign[e_1(t)] - sign[e_1(t) + y'(t)]))sign[e_0(t)]$ is a piece-

wise continuous function (for $\beta > L_1 + L_2 + 2\chi$ it is strictly positive and $0 < \delta \le \gamma(t) \le \kappa$, $\delta = \beta - L_1 - L_2 - 2\chi$, $\kappa = \beta + L_1 + L_2 + 2\chi$, see [24] for more details). Assume that $|v(t)| \le \lambda_0$ for all $t \in R$. By definition $|\delta_0(t)| \le \alpha\sqrt{2\lambda_0}$, $\delta_1(t) = 0$ for $|e_0(t)| \ge \lambda_0$, $|\delta_1(t)| \le 2\beta$ and $\delta_1(t)e_0(t) \ge 0$ for all $t \in R$.

Lemma 1: Global boundedness of solutions
Let the signal $v : R \to R$ *be Lebesgue measurable and* $|y'(t)| \le L_1$, $|y''(t)| \le L_2$, $|v(t)| \le \lambda_0$ *for all* $t \in R$; $\alpha > 0$, $\beta > 0$ *and* $0 < \chi < \beta$. *Then in (4) for all* $t_0 \in R$ *and initial conditions* $z_0(t_0) \in R$, $z_1(t_0) \in R$ *the solutions are bounded*:

$$|z_0(t) - y(t)| < \max\left\{|z_0(t_0) - y(t_0)|, 4\alpha^{-2}(|z_1(t_0) - y'(t_0)| + 3\beta + L_1 + L_2 + \chi + \alpha\sqrt{2\lambda_0})^2\right\}$$

$$|z_1(t) - y'(t)| \le |z_1(t_0) - y'(t_0)|e^{-0.5t} + |3\beta + L_1 + L_2 + \chi|. \quad \blacksquare$$

Proof: Let us start with the second equation in the system (5), considering the Lyapunov function $U(e_1) = 0.5e_1^2$, with the derivative $\dot{U} \le -U + 0.5[3\beta + L_1 + L_2 + \chi]^2$. That gives the desired estimate. Next consider $U(e_0) = 0.5e_0^2$:

$$\dot{U} \le -\alpha\sqrt{|e_0|}|e_0| + |e_0|(|e_1| + \alpha\sqrt{2\lambda_0}).$$

Since $|e_1(t)| \le |e_1(t_0)| + 3\beta + L_1 + L_2 + \chi$ for $|e_1(t_0)| + 3\beta + L_1 + L_2 + \chi + \alpha\sqrt{2\lambda_0} \le 0.5\alpha\sqrt{|e_0|}$ we have $\dot{U} \le -0.5\alpha\sqrt{|e_0|}|e_0| < 0$, that implies the lemma 1.

Considering now the accuracy of derivatives with non-differentiable noise, let the signal $v : R \to R$ be Lebesgue measurable and $|v(t)| \le \lambda_0$ for all $t \in R$.

Theorem 1.
Let $\beta > L_1 + L_2 + 2\chi$, $\chi > 0$ *and* $\alpha \ge 2\{\sqrt{8\kappa}\chi + \sqrt{\chi(\chi+\kappa)}(\kappa - \delta)\}/(1.5\delta + 0.5\kappa)$, *then for any initial conditions* $\mathbf{e}(0) \in \Omega_0$, $\Omega_0 = \{\mathbf{e} \in R^2 : \kappa|e_0(0)| + 0.5e_1^2(0) \le 2 \times \sqrt{2\kappa(\chi+\kappa)\chi}\delta(\kappa - \delta)^{-1}\}$ *the trajectories of the system (5) satisfy the estimate for all* $t \ge T$

$$|e_0(t)| \le \delta^{-1}(c_1\lambda_0 + c_2\sqrt{\lambda_0}),\ |e_1(t)| \le \sqrt{2(c_1\lambda_0 + c_2\sqrt{\lambda_0})},$$

$$c_1 = \max\{8\mu^{-2}[(0.25\delta + \kappa)\alpha + \max\{\sqrt{2(\chi+\kappa)}, 6\}\beta]^2, \kappa\},$$

$$c_2 = \beta^2/(\alpha\sqrt{2}),\ \mu = \min\{\alpha\delta/\sqrt{\kappa}, \sqrt{2}\chi\},$$

where the finite time T *of convergence possesses the estimate* $T \le 4\mu^{-1}\sqrt{\kappa|e_0(0)| + 0.5e_1^2(0)}$, *provided that*

$$c_1\lambda_0 + c_2\sqrt{\lambda_0} \le 2\sqrt{2\kappa(\chi+\kappa)}\chi\delta(\kappa - \delta)^{-1}. \quad \blacksquare$$

Proof: see [24]

Theorem 1 is based on the observation that δ_1 (the product $e_1\delta_1$) influences negatively on (5) onto the set $\Gamma = \{|e_0| < \lambda_0 \wedge 3\alpha\sqrt{2\lambda_0} < |e_1| < 2\beta \wedge e_0e_1 > 0\}$ only.

The result of the theorem says that if the noise amplitude λ_0 is comparable with the chosen α, β, χ (the constraint $c_1\lambda_0 + c_2\sqrt{\lambda_0} \le 2\sqrt{2\kappa(\chi+\kappa)} \times \chi\delta(\kappa-\delta)^{-1}$ holds), then the estimate on the derivative y' has the error proportional to $\lambda_0^{0.25}$ (theoretical limitations of this estimate improvement are established in [32]). If the noise amplitude is very high, then the result of lemma 1 is satisfied guaranteeing boundedness trajectories. It is worth to stress, that the value $2\sqrt{2\kappa(\chi+\kappa)} \times \chi\delta(\kappa-\delta)^{-1}$ can be taken arbitrary high adjusting α, β, χ.

Remark 1: A trade-off between the finite-time of convergence and the accuracy of derivate must be done by means of the tuning parameters α, β and χ achieving $\beta > L_1 + L_2 + 2\chi$ and $\alpha \ge 2\{\sqrt{8\kappa\chi} + \sqrt{\chi+\kappa}(\kappa-\delta)\}/(1.5\delta + 0.5\kappa)$ with $\delta = \beta - L_1 - L_2 - 2\chi$ and $\kappa = \beta + L_1 + L_2 + 2\chi$. A gridding-based optimization procedure [28] can be used but for brevity, the procedure is not given in this paper.

3.2. Fault reconstruction

The estimation algorithm design for the fault signal f reconstruction is performed in two steps in this sub-section. Firstly, the main assumptions are introduced. Secondly, a hybrid algorithm is presented and its conditions of convergence and accuracy are analyzed.

Assume that the system (1)–(3) state belongs to some compact set.

Assumption 1. *Let* $(y(t), y'(t)) \in Y \subset R^2$ *for all* $t \ge 0$. □

This assumption is quite realistic. Typically, the set Y is known and predefined during the design phase. When the faults f are present, the system (2) may lose its stability. However, as it will be shown below even in this case the algorithm requires a finite time to detect the fault. Hence, recovery actions can be made to maintain stability and some pre-defined performance level [25, 28, 34].

According to theorem 1, for the system (1)–(4) there exists a finite time T of convergence $T \le 4\mu^{-1}\sqrt{\kappa|e_0(0)| + 0.5e_1^2(0)}$ such that $y^{(k)} = z_k(t) - e_k(t)$, with $|e_0(t)| \le \delta^{-1}(c_1\lambda_0 + c_2\sqrt{\lambda_0})$ and $|e_1(t)| \le \sqrt{2(c_1\lambda_0 + c_2\sqrt{\lambda_0})}$ for all $t \ge T$. Then, the system (2) can be presented as follows

$$z_1(t) - e_1(t) = F(t, z_0(t) - e_0(t), u(t)), \ t \ge 0, \tag{6}$$

Let $Y_\upsilon \subset R^2$ be the neighborhood of the set Y ($Y \subset Y_\upsilon$) such that if $|z_0(t) - y(t)| \le \delta^{-1}(c_1\lambda_0 + c_2\sqrt{\lambda_0})$, $|z_1(t) - y'(t)| \le \sqrt{2(c_1\lambda_0 + c_2\sqrt{\lambda_0})}$ and $(y, y') \in Y$, then necessarily $(z_0, z_1) \in Y_\upsilon$. Since the function F is locally Lipschitz continuous then for all $(z_0, z_1) \in Y_\upsilon$ there exists $L > 0$ such that

$$|F(t, z_0(t) - e_0(t), u(t)) - F(t, z_0(t), u(t))| \le L|e_0(t)|$$

According to theorem 1 we have $|e_0(t)| \le \delta^{-1}(c_1\lambda_0 + c_2\sqrt{\lambda_0})$ for all $t \ge T$. Therefore, from the expression (6) we can define the augmented error

$$\begin{aligned}\delta(t) &= z_1(t) - F(t, z_0(t), u_0(t) + f(t)) \\ &= F(t, z_0(t) - e_0(t), u(t) + f(t)) + e_1(t) - F(t, z_0(t), u_0(t) + f(t))\end{aligned} \tag{7}$$

with $|\delta(t)| \le \rho(\|v\|)$ for all $t \ge T$,

$$\rho(s) = L\delta^{-1}(c_1 s + c_2\sqrt{s}) + \sqrt{2(c_1 s + c_2\sqrt{s})}\ .$$

All variables in the right hand side of (7) are available for measurements except the fault signal $f(t)$. In the left hand side of (7) we have the augmented error δ, that represents the accuracy of the derivative estimation by the differentiator (4), it is not measurable and it is proportional to the measurement noise v amplitude (this error becomes zero in the finite time T for the case of no measurement noise). Let $\hat{f}(t)$ be a solution of the equation (7) for the case $\delta(t) = 0$, i.e.

$$z_1(t) = F(t, z_0(t), u_0(t) + \hat{f}(t))\ . \tag{8}$$

then substituting (8) in (7) we get

$$\delta(t) = F(t, z_0(t), u_0(t) + \hat{f}(t)) - F(t, z_0(t), u_0(t) + f(t))\ .$$

Define the gradient of the function F with respect to u

$$\nabla_u F(t, y, u) = \partial F(t, y, u)/\partial u\ ,$$

then by the Mean value theorem there exists a function $c : R_+ \to [0,1]$ such that for all $t \ge 0$

$$\delta(t) = g(t)[\hat{f}(t) - f(t)]\ . \tag{9}$$

$$g(t) = \nabla_u F(t, z_0(t), u_0(t) + [1 - c(t)]\hat{f}(t) + c(t) f(t))\ .$$

Assumption 2. *Let*

$$\int_0^t |\, g(\tau)[\hat{f}(\tau) - f(\tau)]\,|\, d\tau \ge g_{\min} t\, |\, \hat{f}(t) - f(t)\,|^p\ .$$

for all $t \ge T$ *and some* $g_{\min} > 0$, $0 < p < +\infty$. □

The condition of the assumption 2 means that on the time interval $t \ge T$ the integral $\int_0^t |\, g(\tau)^T [\hat{f}(\tau) - f(\tau)]\,|\, d\tau$ has average value bigger than $g_{\min}\, |\, \hat{f}(t) - f(t)\,|^p$. Roughly speaking this property says that the function $g : R_+ \to R$ norm has strictly separated from zero average value for all $t \ge T$. This property can also be considered as a variant of the well known persistency of excitation condition in the estimation theory [29]. Then under assumption 2 from (9) for all $t \ge T$

$$\rho(\|v\|)t \ge \int_0^t |\delta(\tau)| d\tau = \int_0^t \left| g(\tau)[\hat{f}(\tau) - f(\tau)] \right| d\tau \ge g_{\min} t \left| \hat{f}(t) - f(t) \right|^p\ .$$

and finally,

$$|\, \hat{f}(t) - f(t)\,| \le [\, g_{\min}^{-1} \rho(\|v\|)\,]^{1/p}\ ,$$

that implies boundedness of the discrepancy $\hat{f}(t) - f(t)$ for all $t \ge T$. In other words, accuracy of the fault signal f estimation by $\hat{f}$ is a function of the meas-

urement noise v amplitude. Consequently, under assumption 2 the problem of fault detection and isolation can be handled finding a solution $\hat{f}$ of the equation (8), the penalty is proportional to $\| v \|$.

The equation (8) is nonlinear, for each $t \geq 0$ it may have a single solution $\hat{f}(t)$ or in general case, $\hat{f}(t) \in S_t$, where for all elements $s \in S_t$ the equation

$z_1(t) = F(t, z_0(t), u_0(t) + s)$

holds. It could be the case that for some $t \geq 0$ this equation has no solution with respect to $\hat{f}(t)$. Thus, some regularizing conditions have to be imposed.

Assumption 3. *Let* $\nabla_u F(t, z_0(t), u(t)) \neq 0$ *for all* $(z_0, z_1) \in Y_\upsilon$, $u \in R$ *and* $t \geq 0$.□

Note that assumption 3 does not necessarily imply assumption 2. This assumption states that the gradient of the function F with respect to the last argument u is restricted from zero, or in other words, under these restrictions the equation (8) has the single solution $\hat{f}(t)$. Then any gradient descent method (the Newton–Raphson method, …) can be applied to find an estimate $\breve{f}(t)$ on the solution of (8) $\hat{f}(t)$:

$$d\breve{f}(\tau)/d\tau = \gamma\varphi[\sigma(t, \breve{f}(\tau))], \tag{10}$$

$\varphi(s)s > 0$ for all $s \neq 0$, $\| \varphi \| < +\infty$,

$\sigma(t, f) = [z_1(t) - F(t, z_0(t), u_0(t) + f)]\nabla_u F(t, z_0(t), u_0(t) + f)$

where $\gamma > 0$ is a design parameter and $\tau \geq 0$ is an independent time. For each fixed $t \geq 0$ the execution of (10) in the time τ ensures convergence of $\breve{f}(\tau)$ to $\hat{f}(t)$ (more precisely this claim will be formulated later).

Under the introduced assumptions 1-3, the proposed solution consists in discretization of (10), when the estimate $\breve{f}(t_k)$ is generated discretely for some sequence of strictly increasing sample instants t_k, $k \geq 0$ ($t_0 = 0$) having accumulation point at infinity only. Then the discrete representation of (10) can be written as follows for any $k \geq 0$:

$$\theta_0 = \breve{f}(t_k),\ \breve{f}(t_0) = \breve{f}_0; \tag{11}$$

$\theta_{r+1} = \theta_r + \gamma\varphi[\sigma(t_k, \theta_r)]$, $r = \overline{0, N-1}$; $\breve{f}(t_{k+1}) = \theta_N$,

where $\gamma > 0$, $N > 0$ and $\breve{f}_0 \in R$ are design parameters. The operation of (11) can be expressed as follows: at each sampling time t_k the algorithm takes the initial value $\theta_0 = \breve{f}(t_k)$ (or some guess $\theta_0 = \breve{f}_0$ on the first step $k = 0$), then N steps of the discrete minimization procedure (10) are computed, the output of the algorithm (11) is $\breve{f}(t_{k+1}) = \theta_N$. The number N is bounded by available computational power for (11) realization. The system (11) period or the shift between the sample instants $t_{k+1} - t_k$, $k \geq 0$ depends on the time that is required to perform N steps of (11) and the fault detection minimum time specifications. The stability properties of the obtained hybrid system (1)–(4), (11) (its structure scheme is shown in Fig. 2) are analyzed below.

Theorem 2. *Let assumptions 1−3 hold, then in the system (1)−(4), (11) for any* $\varepsilon^* > 0$ *there exist* $\gamma^* > 0$ *and* $N^* \geq 0$ *such that for any* $k > 0$ *with* $t_k \geq T$ *(where* $T \geq 0$ *is the time of the derivatives estimation from theorem 1)*

$$|\breve{f}(t_{k+1}) - f(t_k)| \leq \varepsilon^* + [g_{\min}^{-1}\rho(\|v\|)]^{1/p};$$

provided that $0 < \gamma < \gamma^*$, $N \geq N^*$ *for any initial conditions,* $v \in \mathcal{L}_\infty$ *and continuous* $f \in \mathcal{L}_\infty$.

Proof: See [25]

The result of theorem 2 claims that for any desired accuracy $\varepsilon^* > 0$ there exists some maximum adaptation rate $\gamma^* > 0$ and maximum number of steps $N^* \geq 0$ such that the fault value $f(t_k)$, $t_k \geq T$ for all such $k \geq 0$ is estimated by the algorithm (11) output $\breve{f}(t_{k+1})$ with the worst case accuracy $[g_{\min}^{-1}\rho(\|v\|)]^{1/p} + \varepsilon^*$. In the absence of the measurement noise v the accuracy ε^* is achievable. The theorem does not restrict the sampling rate in the system (the delay $t_{k+1} - t_k$, $k \geq 0$ can be chosen in accordance with computational constraints). There exists a casual time shift in the algorithm response ($\breve{f}(t_{k+1}) \to f(t_k)$) due to calculations in (11) performed on the interval $[t_k, t_{k+1})$, the estimate on the value $f(t_k)$ is always obtained on the next step t_{k+1} only.

In particular, for FDI purposes, if $0 < t_{k+1} - t_k \leq \mathrm{T}_0$ ($\mathrm{T}_0 > 0$ is the maximal sample time of the algorithm (11) operation), then theorem 2 guarantees that for time instants $t_k \geq T + T_0$, $k \geq 0$ the signal $\breve{f}(t_k)$ detects all faults with amplitudes bigger than $[g_{\min}^{-1}\rho(\|v\|)]^{1/p} + \varepsilon^*$ (in other words, $T + \mathrm{T}_0$ is the fault detection time and $[g_{\min}^{-1}\rho(\|v\|)]^{1/p} + \varepsilon^*$ represents the amplitude of the smallest detectable fault).

3.3. Decision making rules used in A380 airplane

As described in [1], the used OFC decision making rule consists in counting successive and alternate crossings of a given threshold η in a sliding time window according to the principle of Fig. 3. The sliding time window is used to count down the oscillation counter in order to avoid cumulating transitory threshold crossings (due to model uncertainties, aerodynamic forces, …) that would necessarily lead to a false alarm. Here, the flight control law unit is considered as fault free process. All its oscillations are judged normal and are calculated to compensate any normal perturbation (*e.g.* an external disturbance such as turbulence). The hypothesis of a fault-free command is justified because the flight control law is also monitored by dedicated techniques.

In the case of liquid failures, the residual is given by

$$r(t_k) = \breve{f}_{liq}(t_k) = \breve{f}_{harm}(t_k) + \xi(t_k)$$

where $|\xi(t_k)| \leq \varepsilon^* + [g_{\min}^{-1}\rho(\|v\|)]^{1/p}$. After the filtering given in [1], the residual is zero-averaged and OFC can be detected by counting around zero alternate and successive crossings of a threshold (see Fig. 3).

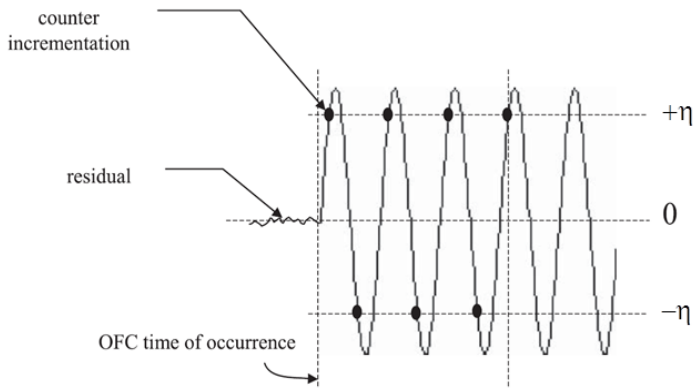

Figure 3. OFC detection by oscillation counting

In case of a solid failure, the OFC substitutes the nominal signal. The residual is expressed as

$$r(t_k) = \breve{f}_{sol}(t_k) = \breve{f}_{harm}(t_k) - \breve{u}_0(t_k) + \xi(t_k)$$

If the estimated position is null (no control surface deflection) the residual is only composed of the failure and bounded error ξ. OFC detection can be thus done by oscillation counting around zero, like for the liquid failure. However, if a control surface deflection is demanded by the flight control law (e.g. during a maneuver or in reaction to the failure), the failure signal is mixed with the opposite of the estimated position, and an oscillation counting around zero would not enable detection. In this case, it is proposed to count OFC on the residual signal but around the opposite of the estimated position. The interested reader can refer to [1] for more details. Note that both liquid and solid OFC countings operate in parallel.

Remark 2. Note that if it is desired to design a "dedicated" FDD scheme for any kind of failure in the actuator control loop, the decision rule could be a simple threshold-based logic. However, the goal here is to detect, and further to confirm that the fault to be detected is an OFC, and not something else. This is why the above evaluation rule is used.

Remark 3. In the following, the minimum confirmation time is set to 3 cycles [26], and the question is: given the specified flight conditions, if an OFC occurs (small amplitude and different frequencies) at different time instants, can oscillatory phenomenon be detected to confirm its presence in less than 3 cycles, without any false alarm and missed detection?

4. Experimental results

Two validation tools are used to assess the hybrid monitoring scheme. The first set of simulation results uses a high fidelity aircraft benchmark provided by Air-

bus [33] during ADDSAFE project. The proposed technique is next evaluated on a dedicated Functional Engineering Simulator (FES) developed also during the ADDSAFE project for more detailed evaluation in a Monte-Carlo setup [7, 30]. This simulator developed by Deimos Space covers all possible flight conditions, perturbations and parametric uncertainties [30]. It is an industrial benchmarking where the "Figure Of Merits" (FOM), which are scalar quantities used to characterize the performance of a FDD system, are computed to provide a quantitative benchmarking of the FDD designs based on an Airbus' defined FDD performance and robustness matrix [26].

The control surface considered in this work is the right inboard aileron of a generic Airbus commercial aircraft. The requirement specifications are 0% of missed detection, 0% of false alarm and 100% of true detection for all flight conditions. In this paper, the case study is to detect an OFC in less than 3 cycles. Hence, the decision making rules given in section 3.3 is tuning in order to detect an OFC when two successive periods of oscillation appear on the residuals. Note that for industrial reasons and since it is not of primary interest in this work to give the exact aircraft behaviors, all simulation results have been normalized.

4.1. Airbus benchmark results

The Airbus benchmark [33] is a complete aircraft model, highly representative of a generic twin engine civil commercial aircraft including the nonlinear rigid-body aircraft model with a full set of control surfaces (rudder, elevators, Trimmable Horizontal Stabilizer, spoilers, ailerons), actuator models, sensor models, flight control laws and pilot inputs. It is a closed loop non linear model with five main components: pilot inputs, flight control laws, actuators, aircraft and sensors. It has been developed under Matlab/Simulink environment and is usable under the same software thanks to dedicated Graphical User Interfaces (GUI).

The actuator modeling is based on three elements: the actuator model itself, a control surface position saturation that could be dissymmetric and a rate limiter representing the physical limitations. The model input is a commanded actuator position (output of the flight control law computation) while the output is a realized actuator position. The pilot inputs are the side stick (longitudinal and lateral inputs), the pedals, the high-lift configuration lever (slats and flaps), the airbrakes and the throttle lever. Flight control law is a gain scheduled control to cover the whole flight domain. Finally, the aircraft unit is based on the classical flight mechanics modeling where both quaternion system and Euler angle formulation are used.

To assess the potential of our FDD scheme, six different flight maneuvers (Nose up, Angle of attack protection, Pitch protection, Yaw angle mode, Turn coordination and Cruise scenarios) are simulated for fault-free situations. The

aforementioned flight scenarios are used to show the good robustness and performances of our FDD scheme for both lateral and longitudinal modes.

Let the robustness of the proposed FDD scheme be now studied. It follows that the amplitude of residual stays small for five flight maneuvers (see Fig. 4). For the yaw angle mode scenario, a dynamic phase introduces some dynamic behavior of the residual due to an important variation in the aerodynamic forces. Since it is necessary to have two successive periods of oscillation to detect a fault, our algorithm concludes well to a nominal (no fault) situation, *i.e.* no fault is detected. Hence, the proposed residual generation fitted to the decision block shown in section 3.3 gives no false alarm. Note that the noise of the residual is proportional to the noise used in the benchmark ADDSAFE that is an inherited feature after the differentiator (see Theorem 1).

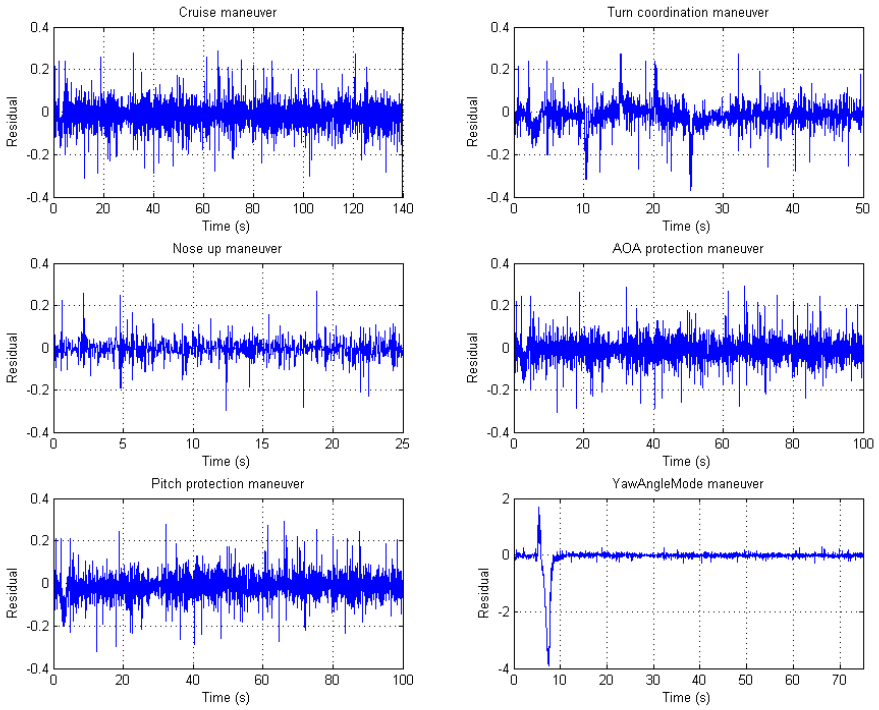

Figure 4. Robustness analysis - normalized residuals on right inboard aileron

Several OFC amplitudes and frequencies have now been tested for both liquid and solid OFC. In all cases, the oscillatory phenomenon appears clearly on residual signal and the fault is detected by the decision block. Due to space limitation, no plot is given in this subsection to highlight in more details the benefit of the

hybrid monitoring scheme with parametric variations. However, it appears for all tests, we get 100% of true detection and 0% of missed detection.

4.2. FES parametric simulation results

In fault-free situations, the tests were conducted for the six previous flight scenarios with variations in the operating conditions and uncertainties. The simulation campaign for one flight maneuver has been defined with 324 simulations runs [30] resulted from the combination of the following parameters:

- altitude: h = [8000 18000 28000 38000] ft;
- calibrated air-speed: V_{CAS} = [160 220 300] kts;
- mass: m = [120000 180000 233000] kg;
- X-component of gravity center: [0.17 0.3 0.41] %/100

For each combination of these flight and aircraft parameters, three additional variations (minimum, nominal and maximum errors or uncertainties) associated with the aerodynamic coefficients and sensors measurements have also been included. In ADDSAFE project, only realistic operating points belonging to the flight envelop are taken into account within the Figures Of Merit (FOM, see [26]), i.e. only realistic situations are used to assess our FDD scheme.

Fig. 5 shows the residuals obtained in FES environment for healthy situations where no fault is detected. The results show a good robustness against parametric variations since the FOM give 0% of false alarm for the 1200 realistic fault free simulation runs. In addition, it is interesting to note that the parametric tests involve some unwanted oscillatory behaviors of residuals between 0 and 5 seconds (see the yaw angle mode maneuver of Fig. 5). These behaviors are due to the command signal generated by the flight control unit. On the other hand, some normal oscillations with the frequency between 0.1Hz and 1 Hz can be observed in addition to the faults to be detected, making the detection of OFC more difficult. Hence, in this situation, the detection threshold of the decision block has to be set to a higher value to keep 0% of false alarm.

Now, let's take a look to the faulty situation with the parametric variations. Due to important numbers of data generated during the simulations, only the results corresponding to the smallest OFC amplitude and the minimal and maximal considered OFC frequencies (0.5 and 7Hz respectively) are given. Figures 6 show the normalized residuals for liquid (left part) and solid (right part) faults respectively. As it can be seen, the residual is small before the fault occurrence for both liquid and solid faulty situations. Next, a significant change of the residual appears. For the liquid faults, the residual is a noisy sinusoid where the frequency of this sinusoid coincides with the frequency of the fault (see Fig. 6). In all cases, there is no missed detection. The statistical results given by FOM for the smallest OFC amplitude (Airbus specifications, not given here for industrial reasons), all types (liq-

uid or solid) and the two extreme frequencies of OFC faults are summarized in Table 1. The detection time performance (DTP) index is used to quantify the detection delay requirement in a normalized way, i.e. $DTP < 1$ denotes an enhancement of detection delay, $1 < DTP < 1.3$ represents an acceptable level of performances and $DTP > 1.3$ is judged like unacceptable detection delays. These indexes are next used by a normalized cost function [26] (not given in this paper for confidentiality reasons). It is obvious that in the assessment of the FDI scheme, a index $DTP < 1$ has a better weighting performance index than $DTP > 1.3$. From Table 1, OFCs are always detected with satisfactory detection time, i.e. we obtained 100% of true detection and so 0% of missed detection for the considered flight maneuvers with acceptable detection delays.

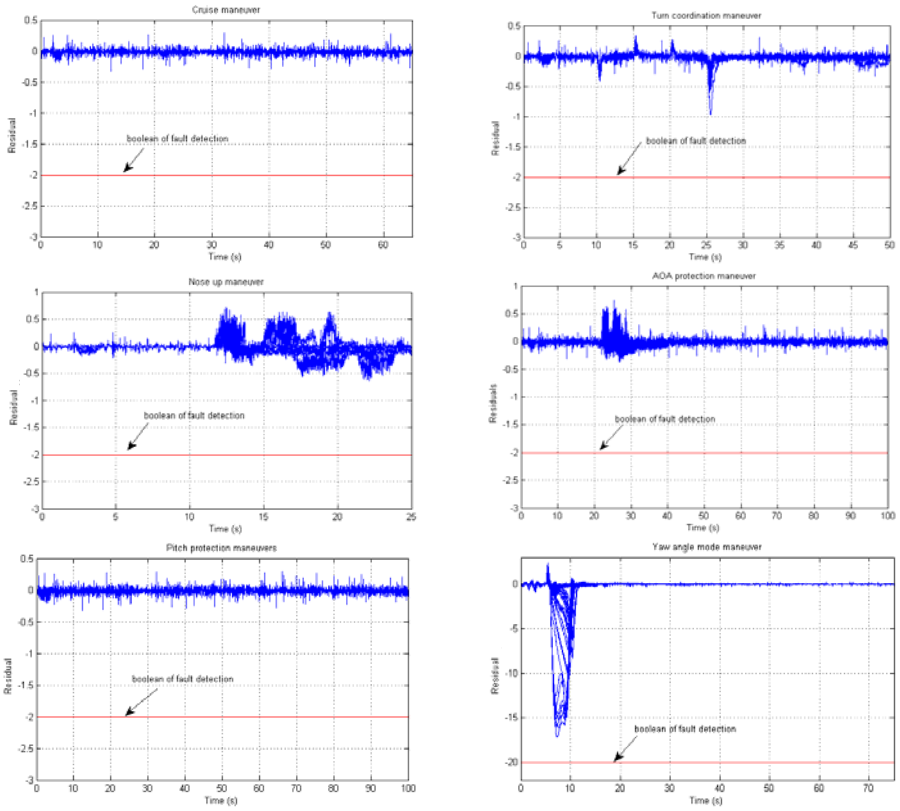

Figure 5. Normalized residuals in fault-free situations – parametric variations

4.3. Implementation aspects

The proposed scheme is coded using a restricted symbol library provided by Airbus [26]. The low computational complexity of the proposed detection method allows for developing a scheme that is only based on 322 basic operators like de-

lays, multiplications, additions, gains, sign function, look up tables, logic operators. The computational load can thus be evaluated by using the running time of each symbol. It follows that the proposed strategy uses only 47% of computing cost allowed.

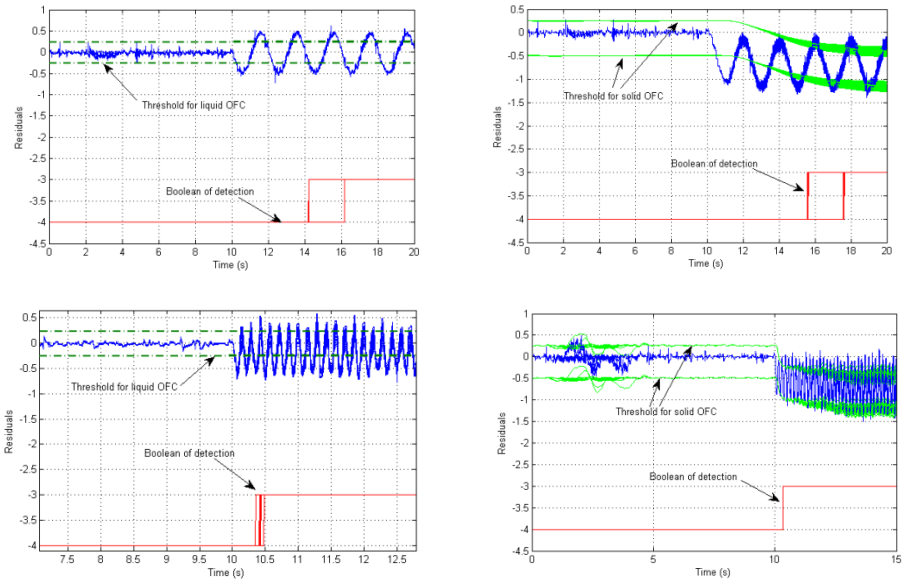

Figure 6. Normalized residuals for liquid (left) and solid (right) fault

4.4. Discussion

Simulation results show the benefits of a combination of the proposed hybrid monitoring scheme and OFC decision making rules. The proposed hybrid monitoring scheme seems to be a good and technologically viable candidate to achieve OFC detection in noisy environment with acceptable detection delays.

Table 1: FOM for OFC fault in the right inboard aileron – parametric tests

Type	Amp	*f* (Hz)	Normalized Detection Time Performance			True det. (%)	Missed det. (%)
			Mean	Max	Min		
Liquid	**smallest**	**0.5**	0.747	1.03	0.7	100	0
Solid	**smallest**	**0.5**	1.06	1.27	0.93	100	0
Liquid	**smallest**	**7**	0.9471	1.12	0.84	100	0
Solid	**smallest**	**7**	0.79	0.79	0.79	100	0

Another interesting feature of this work is relative to the robustness of the hybrid monitoring against other types of fault (see remark 2). One of the benchmark problem considered in ADDSAFE is a scenario involving abnormal aircraft behaviors that lead to the degradation of the aircraft performance [26, 30, 31]. In this case, Figures 9 show the results of control surface liquid and solid jamming [31] with parametric variations. Simulation results show that the proposed monitoring scheme is not sensitive to such type of faults. It is a great feature of the proposed work since a simple threshold-based logic will conclude to fault detection, i.e. there is no robustness against liquid and solid jamming.

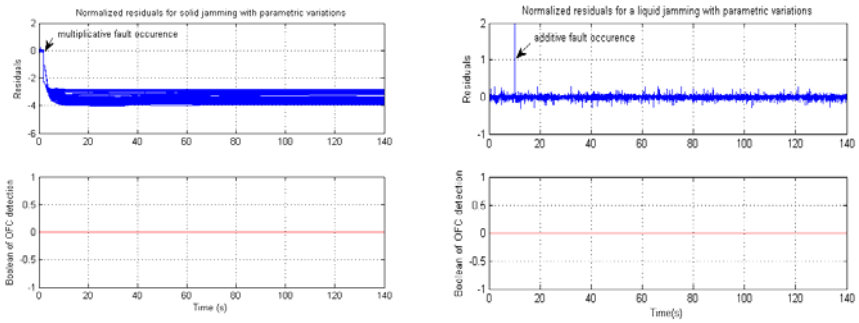

Figure 9. Normalized residual for solid (right) and liquid (left) jamming with parametric variations

5. Conclusion

The problem studied in this paper is that of designing a robust detection unit for early detection of OFC that can occur in EFCS of civil aircraft. The motivation behind this work is that for upcoming and future aircraft programs, it could be required to detect unauthorized oscillatory events in control surfaces servo-loops with less important amplitude in less time while keeping a good robustness. The final goal is to avoid reinforcing the structure and consequently to save weight. The paper presents hybrid solution fitted to the in-service A380 decision making rules to solve the above problem. Experimental results suggest that the proposed hybrid differential observer could be a suitable candidate for in board implementation in flight computers. A number of appealing avenues can be considered for further investigations. For example, further investigations are necessary to adapt the monitoring procedure for new generation Electrohydrostatic Actuator (EHA) and Electro-Backup-Hydrostatic Actuator (EBHA) which are used on A380 airplane.

Acknowledgments

This work was performed in the framework of the European ADDSAFE project: grant agreement n° FP7-233815.

References

[1] Goupil P., 'Oscillatory failure case detection in the A380 electrical flight control system by analytical redundancy', Control Engineering Practice, 2010, **18**(9), pp. 1110−1119.

[2] Goupil P., 'Airbus state of the art and practices on FDI and FTC in flight control system', Control Engineering Practice, 2011, **19**(6), 524-539.

[3] Alcorta Garcia, E., Zolghadri, A., Goupil, P., 'A Nonlinear Observer-Based Strategy for Aircraft Oscillatory Failure Detection: A380 Case Study', IEEE Transactions on Aerospace and Electronic Systems, 2011, **47**(4), 2792-2806.

[4] Zolghadri A., Gheorghe A., Cieslak J., Henry D., Goupil P., Dayre R., Le Berre H., 'A Model-based Solution to Robust and Early Detection of Control Surface Runaways', SAE Int. Journal of Aerospace, November 2011 **4**:1500-1505.

[5] Berdjag D., Cieslak J., Zolghadri A., 'Fault diagnosis and monitoring of oscillatory failure case in aircraft inertial system', Control Engineering Practice, **20**(12), 2012, 1410-1425, http://dx.doi.org/10.1016/j.conengprac.2012.08.007.

[6] Edwards C., Lombaerts T., Smaili H., 'Fault Tolerant Flight Control: a benchmark challenge', Lecture Notes in Cont. & Info. Sciences, 2010, Springer.

[7] Goupil P., Marcos A., 'Advanced diagnosis for sustainable flight guidance and control: the European ADDSAFE project', SAE Aerotech congress & exhibition, 2011.

[8] Lavigne L., Zolghadri A., Goupil P., Simon P., 'A model-based technique for early and robust detection of oscillatory failure case in A380 actuators', Int. J. of Control, Automation and Systems, 2011, **9**(1), 42-49.

[9] Sachs H., 'Fault investigation and robust failure detection of oscillating aircraft actuation systems using analytical redundancy', Shaker verlag GmbH, 2010.

[10] Bejarano F.J., Fridman L., Poznyak A., 'Unknown input and state estimation for unobservable systems'. SIAM J. Control Optim., 2009, **48**(2), 1155–1178.

[11] Ferreira A., Bejarano F.J., Fridman L., 'Output hierarchical super twisting observation based robust feedback control: With or without chattering?' Proc. IEEE 46th Conference on Decision in Control, New Orleans, 2007, pp. 4335-4340.

[12] Floquet T., Edwards C., Spurgeon S., 'On sliding mode observers for systems with unknown inputs', Int. J. Adapt. Control Signal Process., 2007, **21**, pp. 638–656.

[13] Fridman L., Shtessel Y., Edwards C., Yan X.-G., 'Higher-order sliding-mode observer for state estimation and input reconstruction in nonlinear systems', Int. J. Robust and Nonlinear Control, 2008, **18**(4-5), pp. 399−413.

[14] Saif M., Xiong Y., 'Sliding mode observers and their application in fault diagnosis'. In Fault Diagnosis and Fault Tolerance for Mechatronic Systems: Recent Advances, 2003, Springer, Berlin, pp.1–57.

[15] Tan C., Edwards C., 'Sliding mode observers for robust detection and reconstruction of actuator and sensor faults', Int. J. Robust Nonlinear Control, 2003, **13**, pp. 443–463.

[16] Yan X.G., Edwards C., 'Nonlinear robust fault reconstruction and estimation using a sliding mode observer', Automatica, 2007, **43**, pp. 1605–1614.

[17] Aldeen M., Sharma R., 'Estimation of states, faults and unknown disturbances in non-linear systems', Int. J. Control, 2008, **81**, pp. 1195–1201.

[18] Chen X., Fukuda T., Young K.D., 'A new nonlinear robust disturbance observer', Systems&Control Letters, 2000, **41**, pp. 189−199.

[19] Hou M., Patton R.J., 'Input Observability and Input Reconstruction', Automatica, 1998, **34**, pp. 789−794.

[20] Xiong Y., Saif M., 'Unknown disturbance inputs estimation based on a state functional observer design', Automatica, 2003, **39**, pp. 1389–1398.

[21] Shtessel Y., Hall C., Baev S., Orr J., 'Flexible Modes Control using sliding mode observers: application to Ares I', Proceeding of conf. on guidance, navigation and control, 2010, Canada

[22] Wang H., Daley S., 'Actuator Fault Diagnosis: An Adaptive Observer-Based Technique', IEEE Trans. Aut. Control, 1996, **41**, pp. 1073−1078.

[23] Alwi H. & Edwards C., 'Oscillatory failure case detection for aircraft using an adaptive sliding mode differentiator scheme', American control conference, 2011.

[24] Efimov D. & Fridman L., 'A hybrid robust non-homogeneous finite-time differentiator', IEEE Trans. on automatic control, 2011, **56**(5), 1213-1219.

[25] Efimov D., Zolghadri A., Raïssi T., 'Actuators fault detection and compensation under feedback control', Automatica, 2011, **47**, pp. 1699−1705.

[26] Goupil P. & Marcos A., 'Industrial benchmarking and evaluation of ADDSAFE FDD designs', 8th IFAC Symp. on fault detection, supervision and safety of technical processes, 2012.

[27] Cieslak J., Henry D., Zolghadri A., 'Fault Tolerant Flight Control: From Theory to Piloted Flight Simulator Experiments', IET Control Theory & Applications, 2010, **4**(8), 1451-1461.

[28] Efimov D.V., Cieslak J., Henry D., 'Supervisory fault tolerant control with mutual performance optimization', Int. Journal of Adapt. Control & Signal Processing, Online in press in 2012. DOI: 10.1002/acs.2296

[29] Narendra K. S., Annaswamy A. M., 'Stable adaptive systems', New Jersey: Prentice-Hall, Inc, 1989.

[30] Marcos A., 'Application of H-infinity fault diagnosis to ADDSAFE benchmark: the control surface jamming case', AIAA guidance, nav. and cont. conf., AIAA 2011-6677, 2011.

[31] Henry D., Zolghadri A., Cieslak J., Efimov D., 'Fault Detection and Diagnosis in Electrical Aircraft Flight Control System', AIAA guidance, nav. and cont. conf., AIAA 2011-6679, 2011.

[32] Kolmogoroff A.N., 'On inequalities between upper bounds of consecutive derivatives of an arbitrary function defined on an infinite interval', Amer. Math. Soc. Transl., **2**, 1962, pp. 233−242.

[33] Goupil P., Puyou G., 'A high fidelity AIRBUS benchmark for system fault detection and isolation and flight control law clearance', European conference for aerospace sciences (EUCASS), 2011.

[34] Cieslak, J., Henry, D., and Zolghadri, A., "A Methodology for the Design of Active Fault Tolerant Control Systems," 6th IFAC Symposium on Fault Detection, Supervision and Safety of Technical Processes [CD-ROM], Pekin, 2006.